On-site Coulomb energy versus crystal-field splitting for the insulator-metal transition in $La_{1-x}Sr_xTiO_3$

T. Higuchi, D. Baba, T. Takeuchi, and T. Tsukamoto
Department of Applied Physics, Tokyo University of Science, Tokyo 162-8601, Japan

Y. Taguchi and Y. Tokura
Department of Applied Physics, University of Tokyo, Tokyo 113-8656, Japan

A. Chainani
RIKEN, Hyogo 679-5143, Japan

S. Shin
Institute for Solid State Physics, University of Tokyo, Chiba 279-5143, Japan
and RIKEN, Hyogo 679-5143, Japan

(Received 20 February 2003; published 18 September 2003)

The on-site Coulomb energy (U_{dd}) and crystal-field splitting ($10Dq$) of doped Mott-insulator $La_{1-x}Sr_xTiO_3$ have been estimated using resonant soft-x-ray emission spectroscopy (SXES). The Raman scattering of the e_g- and t_{2g}-resonant SXES spectra indicate features due to the d-d transitions corresponding to the $10Dq$ and $U_{dd}/2$, respectively. The U_{dd} is in accord with the energy separation between the lower and the upper Hubbard bands obtained by photoemission and inverse-photoemission spectra. The U_{dd} does not change much around two metal-insulator transitions at $x=0.05$ and 0.95 in $La_{1-x}Sr_xTiO_3$, while the crystal-field splitting increases as a function of x.

DOI: 10.1103/PhysRevB.68.104420 PACS number(s): 78.70.En, 71.27.+a, 79.60.−i

I. INTRODUCTION

It is well known that $La_{1-x}Sr_xTiO_3$ changes from a Mott-Hubbard insulator ($LaTiO_3$) with a d^1 configuration at $x=0$ to a band insulator ($SrTiO_3$) with a d^0 configuration at $x=1$. For a wide range of x values in between ($0.08<n<1$), the series exhibits a paramagnetic (PM) metallic phase.[1] The electrical and magnetic properties have been thoroughly investigated by Zaanen, Sawatzky, and Allen[2] and Tokura and co-workers.[1,3–6] The electrical resistivity in the PM phase exhibits a T^2 dependence, characteristic of an interacting Fermi liquid.[3,6] As x decreases in the PM phase ($0.08<x<1$), the electronic specific heat coefficient γ, which is proportional to the conduction electron effective mass (m^*), is enhanced towards the antiferromagnetic (AF) phase boundary ($x=0.08$). Then, the γ decreases in the AF metallic phase ($0.05<x<0.08$) and the AF insulating phase ($x<0.05$). The enhancement of γ is expected for correlated metals near a metal-insulator (M-I) transition at $x=0.05$, though that is not expected for M-I transition at $x=0.95$. Therefore, the M-I transition is believed to be controlled by the relative magnitudes of the on-site Coulomb energy (U_{dd}) and the one-electron bandwidth (W); the system is metallic when $U_{dd}/W \leqslant 1$ and is an insulator when $U_{dd}/W \geqslant 1$.

Photoemission spectra[7,8] (PES) of the bandwidth-control system $Ca_xSr_{1-x}VO_3$ have indicated that the V $3d$ band is split into the quasiparticle band and the remnant of the Hubbard bands and that spectral weight transfer occurs between them as a function of U/W. This behavior is consistent with the prediction of dynamical mean-field theory (DMFT),[9–14] though the m^* exhibits only a very weak enhancement with increasing U_{dd}/W. However, recent PES measurements in the soft-x-ray region reports that the spectra on $SrVO_3$ and $CaVO_3$ have no difference in U_{dd}/W.[15] On the other hand, the Ti $3d$ band in the PES spectra of $La_{1-x}Sr_xTiO_3$ also shows the same type of splitting into the quasiparticle band and lower-Hubbard band, as has been predicted by DMFT.[16–19] Actually, recent PES studies indicate a change of the U_{dd}/W in $La_{1-x}Sr_xTiO_3$.[18,19] Thus, it is quite important to know the real change of U_{dd}/W in $La_xSr_{1-x}TiO_3$ by bulk sensitive measurements.

In this paper, we present high-resolution soft-x-ray emission (SXES) and x-ray absorption spectra (XAS) of $La_{1-x}Sr_xTiO_3$ ($x=0$,0.10). The purpose of this study is to determine experimentally the magnitudes of the on-site Coulomb energy (U_{dd}) and the crystal-field splitting ($10Dq$) near the Mott transition at $x=0.05$ through the study of d-d transitions. Here, one should remember that SXES is a bulk sensitive measurement, while PES and inverse photoemission spectra (IPES) are surface-sensitive measurements. In large d-band filling region ($x \leqslant 0.10$), the authors reported that the Raman scattering of the t_{2g} resonance SXES spectra, which is attributed to d-d transitions between the lower Hubbard and the quasiparticle bands, reflects the magnitude of the effective $U_{dd}/2$.[20–22] Furthermore, it is also reported that the Raman scattering of the e_g resonance SXES spectra, which is attributed to the d-d transition between the t_{2g} and e_g bands, reflects the magnitude of the $10Dq$. Therefore, we can obtain easily the effective U_{dd} and $10Dq$ near the M-I transition by using this technique. As references, the PES and IPES were also measured on the same samples in order to observe the lower and upper Hubbard bands directly.

II. EXPERIMENT

Samples of $La_{1-x}Sr_xTiO_3$ ($x=0,0.10$) were synthesized by melt-quenching stoichiometric mixture of La_2O_3, TiO_2, and SrO powders in a floating-zone furnace. Special attention was paid to synthesis of the samples with x close to 0 including the sample $LaTiO_3$. Careful precalcining of La_2O_3 (source of La) and a fairly strong reducing condition (40% H_2/Ar) prevented La deficiencies and extra oxygen. The single crystals were characterized by x-ray diffraction analysis.

SXES measurements were carried out at the undulator beamline BL-2C at the Photon Factory (PF) of the High Energy Accelerator Organization (KEK). Synchrotron radiation was monochromatized using a varied-line spacing place grating whose average groove density is 1000 lines/mm. The SXES spectra were measured in the depolarized configuration.[23] The energy resolution was higher than 0.4 eV at $h\nu=450$ eV. The energy axis was calibrated by measuring the $4f$ core level of an Au film deposited *in situ* on the sample substrate.

PES measurements were carried out at the revolving undulator beam line BL-19B at PF of KEK. Photoelectron energies were measured with an electrostatic hemispherical analyzer with a radius of 100 mm. The total energy resolution was approximately 40 meV.

IPES measurements were carried out at the Institute for Solid State Physics, University of Tokyo.[24] A filament-cathode-type electron gun was used for the excitation source. The kinetic energy (E_k) of an electron was calibrated by the electron energy analyzer. The IPES spectra were measured using a soft-x-ray emission spectrometer. The total energy resolution of the experimental system was about 0.4 eV at $E_k=60$ eV.

III. RESULTS AND DISCUSSION

Figure 1(a) shows the Ti $2p$ XAS spectrum of $LaTiO_3$. The spectrum consists of two parts derived from the spin-orbit split of L_3 ($2p_{3/2}$) and L_2 ($2p_{1/2}$) states. They are further split into the t_{2g} and e_g states by the octahedral ligand field. The spectrum is very similar to that reported by Abbate *et al.*,[25] who also showed that the energy position of the t_{2g} subband does not depend much on the Sr doping. However, the intensity of t_{2g} subband increases with increasing Sr content, indicating that the doped holes enter into the bottom of the occupied Ti $3d$ band.[25] The vertical bars, which are labeled from *a* to *e*, indicate the selected photon energies for resonant SXES measurements.

Figure 1(b) shows the Ti $2p$ SXES spectra of $LaTiO_3$ excited at photon energies labeled in Fig. 1(a). It is well known that the Ti $2p$ emission reflects the Ti $3d$ partial density of states. An arrow shown in each spectrum is attributed to elastic scattering of the excitation photon. The elastic peak is enhanced at the excitation energy corresponding to the t_{2g} absorption peak of L_3, spectrum *b* of Fig. 1. Then, the peak intensity decreases with increasing excitation energy for spectra *c* to *e*.

The SXES spectrum excited at $h\nu=480$ eV is an off-resonance spectrum attributed to the normal Ti $3d\rightarrow 2p$ fluorescence spectrum. This spectrum indicates that the Ti $3d$ state hybridizes with the O $2p$ state in the valence band. Four dashed lines (*A*, *B*, *C*, and *D* peaks) show the fluorescence bands. As reference, the PES spectrum of $LaTiO_3$ is also shown above the fluorescence spectrum. It is striking that the energy positions of fluorescence spectrum are in a good agreement with those of the PES spectrum. Therefore, we can estimate that the *D* and *C* peaks correspond to the bonding and nonbonding states of the O $2p$ valence band, and the *A* and *B* peaks correspond to the quasiparticle $3d$ band and lower Hubbard band in the band-gap energy region. Thus, our results show that the qusiparticle and lower Hubbard PES band are real bulk state, since fluorescence spectrum is similar to the PES spectrum.

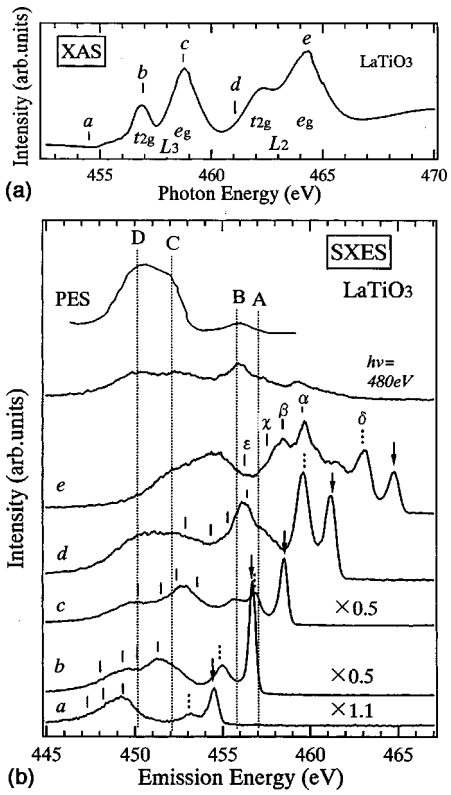

FIG. 1. (a) Ti $2p$ XAS spectrum of $LaTiO_3$. The labels ($a-e$) indicate the photon energies, where the Ti $2p$ SXES spectra were measured. (b) Ti $2p$ SXES spectra excited at various photon energies indicated in (a). Arrow shows the energy position of the excitation photon energy. Vertical lines show the energy positions of Ti $3d\rightarrow 2p$ fluorescence. As reference, the PES spectrum of $LaTiO_3$ in the valence-band region is shown above the fluorescence spectrum.

Four features shown with vertical bars α, β, χ, and ε represent the energy positions that have energy separation of 5.2, 6.2, 7.2, and 8.3 eV, respectively, from the excitation energy. They shift as the excitation energy is varied. These features are attributed to the soft-x-ray Raman scattering (or inelastic scattering). The soft-x-ray Raman scattering that is excited in the L_3 absorption spectral region overlaps with the Ti $3d\rightarrow 2p$ fluorescence. The SXES spectrum *a* excited just below the Ti $2p$ threshold show an apparent feature at a lower energy than the elastic scattering. Since the excitation

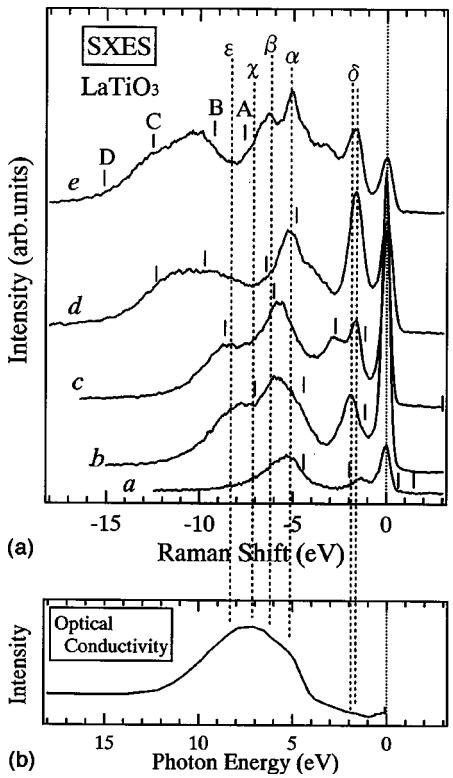

FIG. 2. (a) The Ti $2p$ SXES spectra of $LaTiO_3$ presented on a relative emission energy scale compared to the elastic scattering. (b) The optical conductivity spectrum taken from Ref. 4.

energy is lower than the binding energy, the Ti $3d \rightarrow 2p$ fluorescence cannot be observed. It is attributed to normal Raman scattering, where the intermediate state is a virtual state. Resembling features have been already observed in the SXES spectra of highly doped $La_{0.10}Sr_{0.90}TiO_3$.[20–22]

Figure 2(a) shows the SXES spectra of $LaTiO_3$, where the abscissa is the Raman shift (or energy loss) from the elastic scattering. The elastic scattering peak is located at 0 eV. The Ti $3d \rightarrow 2p$ fluorescence peaks shown by four vertical bars shift to the higher energy with increasing excitation energy. Four dashed lines α, β, χ, and δ indicate the Raman scatterings. These Raman scatterings can be compared with the optical conductivity spectrum,[4] since the elementary excitation of the Raman scattering is the valence-band transition. Therefore, the optical conductivity spectrum of $LaTiO_3$ is shown in Fig. 2(b). Comparing with the SXES spectra, four Raman scatterings are in good accordance with the optical conductivity spectrum, as shown by four dashed lines. This fact indicates that these Raman scatterings are attributed to a charge-transfer (CT) transition from the occupied O $2p$ state to the unoccupied Ti $3d$ state.[20–22] Similar Raman scatterings, which correspond to α, β, and δ of $LaTiO_3$, have been observed in the SXES spectra of $La_{0.10}Sr_{0.90}TiO_3$.[20] However, these energy positions are different from those of $La_{0.10}Sr_{0.90}TiO_3$, indicating the slight change of the band structure.

Figure 3 shows the SXES spectra for Sr doping dependence of $La_{1-x}Sr_xTiO_3$ at the e_g resonance of Ti. These intensities are normalized by the beam current and measurement time. The features from A to D are the Ti $3d \rightarrow 2p$ fluorescence peaks, as shown in Fig. 1(b). The features from α to ε are the Raman scatterings by the CT transition, as shown in Fig. 2(a). In the band-gap energy region, the δe_g peak is observed and its relative intensity decreases with increasing Sr dopant concentration. The Raman shift corresponds to the transition from the occupied t_{2g} subband to the unoccupied e_g subband as indicated by the inset of Fig. 3. That is, the energy position of the d-d transition represents the magnitude of the crystal-field splitting ($10Dq$). The $10Dq$ from e_g-resonance SXES spectra refers to the crystal field in the ground state without the core hole. This is a contrast to the $10Dq$ obtained from the XAS that contains the strong effect of the core hole potential.

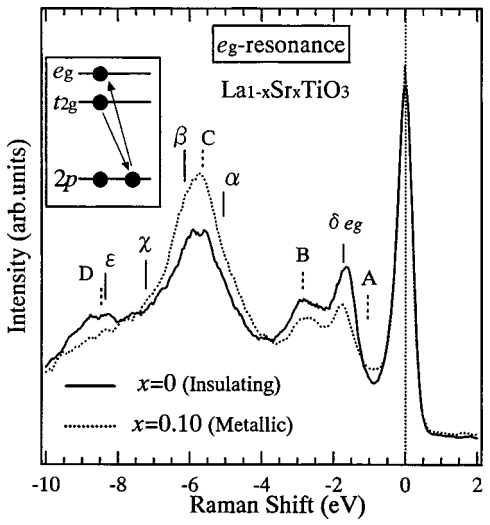

FIG. 3. (a) e_g-resonance SXES spectra of $La_{0.90}Sr_{0.10}TiO_3$ and $LaTiO_3$. The e_g spectrum for $LaTiO_3$ is spectrum c in Fig. 1(b).

Figure 4 shows the SXES spectra as the Sr doping dependence of $La_{1-x}Sr_xTiO_3$ at the t_{2g} resonance of Ti. Comparing each spectrum, the intensity of the δt_{2g} peak in the band

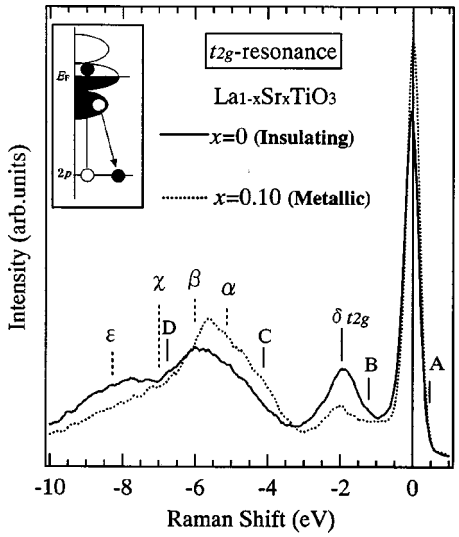

FIG. 4. t_{2g}-resonance SXES spectra of $La_{0.90}Sr_{0.10}TiO_3$ and $LaTiO_3$. The t_{2g} spectrum for $LaTiO_3$ is spectrum b in Fig. 1(b).

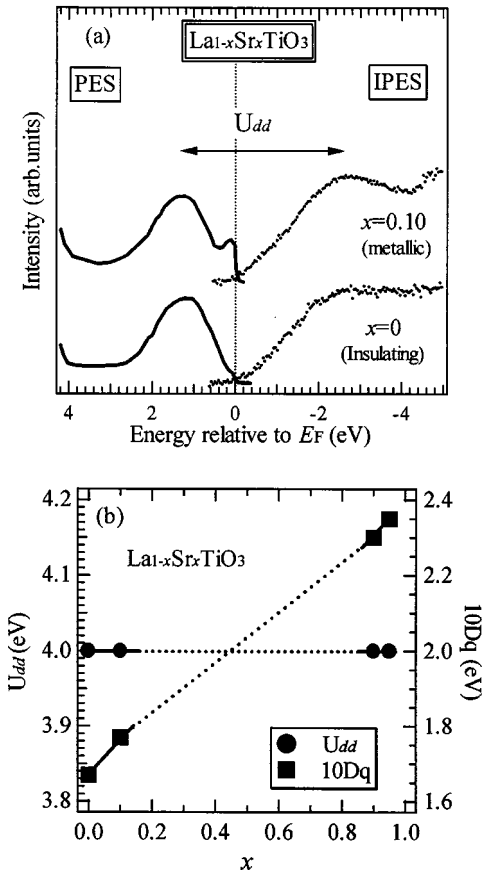

FIG. 5. (a) PES and IPES spectra of $La_{0.90}Sr_{0.10}TiO_3$ and $LaTiO_3$. (b) The crystal-field splitting $(10Dq)$ and U_{dd} as a function of Sr dopant concentration estimated from Figs. 3 and 4. The values for $x=0.90$ and 0.95 are obtained from Ref. 20.

gap decreases with Sr doping. This behavior is in accordance with the change in the intensity of the lower Hubbard band, which has been already observed in the PES spectra. In the case of t_{2g} bands, there is typically no large band splitting so that the contribution to the Raman scattering is due to the on-site electron correlation energy as indicated by the inset. That is, the Raman scattering of the δt_{2g} peak at $\sim$2.0 eV corresponds to the d-d transition from the lower Hubbard band to the unoccupied quasiparticle band. Therefore, we can easily estimate the half on-site electron correlation energy $(U_{dd}/2)$, so that we can experimentally know that the effective U_{dd} does not depend on the Sr dopant concentration.

Figure 5(a) shows the combined PES and IPES spectra of $LaTiO_3$ and $La_{0.90}Sr_{0.10}TiO_3$. The PES spectra have two features in the band-gap energy region below the Fermi level (E_F) that correspond to the quasiparticle band at E_F and to the lower Hubbard band at $\sim$1.3 eV. In the IPES spectra, the prominent peak at $\sim$2.7 eV and a shoulder at 1.0 eV are assigned the upper Hubbard band and quasiparticle band, respectively. The intensity of upper Hubbard band increases and that of quasiparticle band decreases in $LaTiO_3$. These intensity changes of the PES and IPES spectra accord with that of δt_{2g} peak in Fig. 4. These observations are the evidence that the Ti $3d$ spectral weight is transferred from the quasiparticle band to the lower and upper Hubbard bands. On the other hand, the energy separation between the lower Hubbard band and the upper Hubbard band reflects the magnitude of U_{dd}. The estimated $U_{dd}\sim$4.0 eV in both $LaTiO_3$ and $La_{0.90}Sr_{0.10}TiO_3$ is in accordance with the SXES results of Fig. 4. Figure 5(b) shows the $10Dq$ and U_{dd} estimated from Figs. 3 and 4, respectively, as well as from earlier studies of the highly doped samples.[20] The U_{dd} does not change much as a function of hole dopant concentration. On the other hand, the estimated $10Dq$ increases with increasing Sr dopant concentration. This fact agrees with the change in lattice constant. The lattice constant increases due to the distortion related to the increase of Ti-O-Ti bond angle. These facts suggest that the bandwidth also increases with increasing Sr dopant concentration.

IV. CONCLUSION

Our results are in good agreement with the prediction of DMFT calculations. Two *M-I* transitions around $x=0.05$ and 0.95 in $La_{1-x}Sr_xTiO_3$ are well represented by the change of the bandwidth compared to the electron correlation effect. Raman scattering of the e_g and t_{2g}-resonant SXES spectra can be reliably used to quantify the crystal-field splitting $(10Dq)$ and the on-site Coulomb interaction, respectively.

ACKNOWLEDGMENTS

This work was partially supported by the Sumitomo Foundation, and the Grant-In-Aid for Scientific Research from the Ministry of Education, Cultures, Sports, Science and Technology.

[1] M. Imada, A. Fujimori, and Y. Tokura, Rev. Mod. Phys. **70**, 1039 (1999).
[2] J. Zaanen, G. A. Sawatzky, and J. W. Allen, Phys. Rev. Lett. **55**, 418 (1985).
[3] Y. Tokura, Y. Taguchi, Y. Okada, Y. Fujishima, T. Arima, K. Kumagai, and Y. Iye, Phys. Rev. Lett. **70**, 2126 (1993).
[4] Y. Fujishima, Y. Tokura, T. Arima, and S. Uchida, Phys. Rev. B **46**, 11 167 (1992).
[5] T. Katsufuji, Y. Okimoto, and Y. Tokura, Phys. Rev. Lett. **75**, 3497 (1995).
[6] Y. Taguchi, T. Okuda, M. Ohashi, C. Murayama, N. Mohri, Y. Iye, and Y. Tokura, Phys. Rev. B **59**, 7917 (1999).
[7] K. Morikawa, T. Mizokawa, K. Kobayashi, A. Fujimori, H. Eisaki, S. Uchida, F. Iga, and Y. Nishihara, Phys. Rev. B **52**, 13 711 (1995).
[8] I. H. Inoue, I. Hase, Y. Aiura, A. Fujimori, Y. Haruyama, T. Maruyama, and Y. Nishihara, Phys. Rev. Lett. **74**, 2539 (1995).
[9] H. Kajueter, G. Kotliar, D. D. Sarma, and S. R. Barman, Int. J. Mod. Phys. B **11**, 3849 (1997).

[10] K. Maiti, P. Mahadevan, and D. D. Sarma, Phys. Rev. Lett. **80**, 2885 (1998).
[11] V. S. Oudovenko and G. Kotliar, Phys. Rev. B **65**, 075102 (2002).
[12] X. Y. Zhang, M. J. Rozenberg, and G. Kotliar, Phys. Rev. Lett. **70**, 1666 (1993).
[13] G. Kotliar, E. Lange, and M. J. Rozenberg, Phys. Rev. Lett. **84**, 5180 (2000).
[14] H. Kajueter, G. Kotliar, and G. Moeller, Phys. Rev. B **53**, 16 214 (1996).
[15] A. Sekiyama *et al.*, cond-mat/0206471 (unpublished).
[16] A. Fujimori, I. Hase, H. Namatame, Y. Fujishima, Y. Tokura, H. Eisaki, S. Uchida, K. Takegahara, and F. M. F. de Groot, Phys. Rev. Lett. **69**, 1796 (1992).
[17] A. Fujimori, I. Hase, M. Nakamura, H. Namatame, Y. Fujishima, and Y. Tokura, Phys. Rev. B **46**, 9841 (1992).
[18] A. Fujimori, T. Yoshida, K. Okazaki, T. Tsujioka, K. Kobayashi, T. Mizokawa, M. Onoda, T. Katsufuji, Y. Taguchi, and Y. Tokura, J. Electron Spectrosc. Relat. Phenom. **117–118**, 277 (2001).
[19] T. Yoshida, A. Ino, T. Mizokawa, A. Fujimori, Y. Taguchi, T. Katsufuji, and Y. Tokura, Europhys. Lett. **59**, 258 (2002).
[20] T. Higuchi, T. Tsukamoto, M. Watanabe, M. M. Grush, T. A. Callcott, R. C. Perera, D. L. Ederer, Y. Tokura, Y. Tezuka, and S. Shin, Phys. Rev. B **60**, 7711 (1999).
[21] T. Higuchi, T. Tsukamoto, M. Watanabe, Y. Harada, Y. Tezuka, Y. Tokura, and S. Shin, Physica B **281&282**, 615 (2000).
[22] A. Kotani and S. Shin, Rev. Mod. Phys. **73**, 203 (2001).
[23] Y. Harada, H. Ishii, M. Fujisawa, Y. Tezuka, S. Shin, M. Watanabe, Y. Kitajima, and A. Yagishita, J. Synchrotron Radiat. **5**, 1013 (1998).
[24] K. Kanai and S. Shin, J. Electron Spectrosc. Relat. Phenom. **117–118**, 383 (2001).
[25] M. Abbate, F. M. F. de Groot, J. C. Fuggle, A. Fujimori, Y. Tokura, Y. Fujishima, O. Strebel, M. Domke, G. Kaindl, J. van Elp, B. T. Thole, G. A. Sawatzky, M. Sacchi, and N. Tsuda, Phys. Rev. B **44**, 5419 (1991).